



## Study of the “Fast SCR”-like mechanism of H<sub>2</sub>-assisted SCR of NO<sub>x</sub> with ammonia over Ag/Al<sub>2</sub>O<sub>3</sub>

Dmitry E. Doronkin <sup>a,\*</sup>, Sebastian Fogel <sup>b</sup>, Stefanie Tamm <sup>c,d</sup>, Louise Olsson <sup>c,d</sup>, Tuhin Suvra Khan <sup>e</sup>, Thomas Bligaard <sup>f</sup>, Pär Gabrielsson <sup>b</sup>, Søren Dahl <sup>a</sup>

<sup>a</sup> Center for Individual Nanoparticle Functionality (CINF), Department of Physics, Technical University of Denmark, Fysikvej 307, 2800 Kgs. Lyngby, Denmark

<sup>b</sup> Haldor Topsøe A/S, Nymøllevej 55, 2800 Kgs. Lyngby, Denmark

<sup>c</sup> Competence Center for Catalysis, Chalmers University of Technology, SE-412 96 Göteborg, Sweden

<sup>d</sup> Chemical Reaction Engineering, Chalmers University of Technology, SE-412 96 Göteborg, Sweden

<sup>e</sup> Center for Atomic-scale Materials Design (CAMD), Department of Physics, Technical University of Denmark, Fysikvej 307, 2800 Kgs. Lyngby, Denmark

<sup>f</sup> SUNCAT Center for Interface Science & Catalysis, SLAC National Accelerator Laboratory, Menlo Park, CA 94025, USA

### ARTICLE INFO

#### Article history:

Received 22 September 2011

Received in revised form

15 November 2011

Accepted 24 November 2011

Available online 3 December 2011

#### Keywords:

Ag/Al<sub>2</sub>O<sub>3</sub>

Alumina

NO<sub>x</sub> SCR

Fast SCR

FTIR

### ABSTRACT

It is shown that Ag/Al<sub>2</sub>O<sub>3</sub> is a unique catalytic system for H<sub>2</sub>-assisted selective catalytic reduction of NO<sub>x</sub> by NH<sub>3</sub> (NH<sub>3</sub>-SCR) with both Ag and alumina being necessary components of the catalyst. The ability of Ag/Al<sub>2</sub>O<sub>3</sub> and pure Al<sub>2</sub>O<sub>3</sub> to catalyse SCR of mixtures of NO and NO<sub>2</sub> by ammonia is demonstrated, the surface species occurring discussed, and a “Fast SCR”-like mechanism of the process is proposed. The possibility of catalyst surface blocking by adsorbed NO<sub>x</sub> and the influence of hydrogen on desorption of NO<sub>x</sub> were evaluated by FTIR and DFT calculations.

© 2011 Elsevier B.V. All rights reserved.

### 1. Introduction

Nitrogen oxides (NO<sub>x</sub>) are the most challenging pollutants to address for light-duty diesel vehicles and sophisticated techniques like advanced fuel injection, exhaust gas recirculation (EGR), turbocharging, etc., are used by engine manufacturers to reduce emissions. But NO<sub>x</sub> removal by exhaust aftertreatment is still required due to stricter emission regulations and the trade off between fuel consumption and NO<sub>x</sub> emission, i.e., the price for reducing fuel consumption and CO<sub>2</sub> emission by ~15% equals to ~50% increase in NO<sub>x</sub> emissions [1].

Selective catalytic reduction (SCR) is the leading NO<sub>x</sub> control technique with ammonia as a reductant. Commonly used catalysts are vanadia-based catalysts, Cu and Fe-containing zeolites. However, none of the systems demonstrates high thermal durability together with a good activity throughout a broad temperature region from 150 to 550 °C [1]. This fact explains the reason for the on-going research of novel catalytic systems for NH<sub>3</sub>-SCR, which are supposed to be non-toxic, inexpensive and durable.

Alumina supported metals, such as Ag, In, Sn, etc., [2–5] are known to catalyse NO<sub>x</sub> SCR by hydrocarbons under the conditions of lean-burn engine exhaust. The major drawback of these catalytic systems is their very poor activity at low temperatures. It has been found that addition of hydrogen to the gas feed can substantially improve the low-temperature activity of Ag/Al<sub>2</sub>O<sub>3</sub> [6–8]. Interestingly, several groups have also demonstrated the possibility of Ag/Al<sub>2</sub>O<sub>3</sub> to facilitate SCR of NO<sub>x</sub> by ammonia or urea with co-feeding hydrogen, resulting in nearly 90% NO<sub>x</sub> conversion at temperatures as low as 200 °C [9,10].

Hydrogen for this reaction can be provided on board of the vehicle by two means depending on the used reductant. The required amount of hydrogen can be produced in an on-board fuel reformer without the necessity to change the existing fuel infrastructure. This is convenient for hydrocarbon SCR systems utilizing Ag/Al<sub>2</sub>O<sub>3</sub> catalysts and currently leads to fuel penalties from 5 to 10% [11,12] which might be improved by the optimisation of the system. For the NH<sub>3</sub> SCR applications hydrogen can be produced by cracking of part of the ammonia. Pure NH<sub>3</sub> required for this purpose can be stored on board in form of solid metal ammine salts [13]. The suggested system allows accurate and independent dosing of ammonia to the SCR catalyst and to the cracker where it can be decomposed to form the required hydrogen. Using ammonia for hydrogen storage has earlier been suggested for fuel

\* Corresponding author. Tel.: +45 4525 3275.

E-mail addresses: [dmdo@fysik.dtu.dk](mailto:dmdo@fysik.dtu.dk), [dmitriy.doronkin@gmail.com](mailto:dmitriy.doronkin@gmail.com)  
(D.E. Doronkin).

cell applications but can also be applied for  $\text{NO}_x$  SCR applications [14,15].

There is no general agreement about the necessary concentration of hydrogen for the effective reduction of  $\text{NO}_x$  by ammonia over  $\text{Ag}/\text{Al}_2\text{O}_3$ . One can find  $\text{H}_2:\text{NO}_x$  ratios varying from 5 to 10 in the literature [9,10,16–18] which is a rather high value. However, Shimizu and Satsuma have demonstrated ever increasing  $\text{NO}_x$  reduction rate in the interval of  $\text{H}_2:\text{NO}_x$  ratios from 0 to 50 [17] which makes the choice of  $\text{H}_2$  concentration a matter of finding the optimum between the amount of ammonia spent on hydrogen production and the SCR efficiency. We are considering a  $\text{H}_2:\text{NO}_x$  ratio 2.4 as an optimum in this work.

Hydrogen has also been considered as the only reductant in  $\text{H}_2$ -SCR of  $\text{NO}_x$ , however, currently available catalysts allow effective removal of  $\text{NO}_x$  only when using  $\text{H}_2:\text{NO}_x > 10$  and such amount of hydrogen cannot be produced on board at an affordable price [19–21].

In this work we studied several catalysts: Ag supported on different carriers ( $\gamma\text{-Al}_2\text{O}_3$ ,  $\text{TiO}_2$  and  $\text{ZrO}_2$ ), Sn and In supported on  $\gamma\text{-Al}_2\text{O}_3$  and pure alumina under the conditions of  $\text{H}_2$ -assisted SCR of  $\text{NO}_x$  with  $\text{NH}_3$ . The aim of this study is to investigate the possibility of replacing traditional  $\text{NO}_x$  SCR catalysts by  $\text{Ag}/\text{Al}_2\text{O}_3$  thus obtaining high catalyst activity even at low temperatures. Another goal of the study is to give insight to the mechanistic aspects of  $\text{H}_2$ -assisted  $\text{NO}_x$  SCR by ammonia.

## 2. Experimental

### 2.1. Catalyst preparation

Parent  $\gamma$ -alumina (Puralox SCFa-140, 59 ppm  $\text{Fe}_2\text{O}_3$  content) was kindly provided by SASOL. Prior to its study as a catalyst it was calcined at 550 °C for 4 h in static air.

1% $\text{Ag}/\text{Al}_2\text{O}_3$ , 3% $\text{Sn}/\text{Al}_2\text{O}_3$  and 3% $\text{In}/\text{Al}_2\text{O}_3$  were obtained by incipient wetness impregnation of parent  $\gamma$ -alumina by corresponding amounts of  $\text{AgNO}_3$ ,  $\text{SnCl}_4 \cdot 5\text{H}_2\text{O}$  and  $\text{InCl}_3 \cdot 4\text{H}_2\text{O}$  (all from Sigma-Aldrich) solutions in deionised water. 1% $\text{Ag}/\text{TiO}_2$  and 1% $\text{Ag}/\text{ZrO}_2$  were obtained by incipient wetness impregnation of  $\text{TiO}_2$  (anatase containing 10% $\text{SiO}_2$ ) and  $\text{ZrO}_2$  (E10, Magnesium Elektron Ltd.) by the aqueous solution of  $\text{AgNO}_3$ . After impregnation all catalysts were dried at room temperature overnight and calcined at 550 °C for 4 h in static air.

The calcined catalysts were pressed, crushed and sieved to obtain the fraction 0.18–0.35 mm (mesh 80–mesh 45).

### 2.2. TEM measurements

TEM measurements were carried out in a TECNAI T20 transmission electron microscope equipped with an Oxford Instruments EDX detector. For the measurements the catalyst powder (in a dry form) was dispersed on a copper TEM grid covered with a lacey carbon film. Images were acquired using DigitalMicrograph from Gatan Inc.

### 2.3. Catalytic studies

The catalytic measurements were carried out in a fixed-bed quartz flow reactor (inner diameter = 4 mm) in a temperature programmed mode while the temperature was decreased from 400 °C to 150 °C with a rate 2 °C/min. The temperature was controlled using an Eurotherm 2416 temperature controller with a K-type thermocouple. 45 mg of catalyst was diluted with 100 mg of  $\text{SiC}$  (mesh 60) and placed on a quartz wool bed. The bed height was ~11 mm and the GHSV, calculated using the volume of the pure catalyst was ~110,000  $\text{h}^{-1}$ . The gas composition normally contained 500 ppm NO, 520 ppm  $\text{NH}_3$ , 8.3%  $\text{O}_2$ , and 7% water balanced with

Ar. During some tests 1200 ppm of  $\text{H}_2$  was added to the gas feed. The gas feed was mixed from 2000 ppm NO in Ar, 2000 ppm  $\text{NH}_3$  in Ar, 4000 ppm  $\text{H}_2$  in Ar (Air Liquide), oxygen and argon (AGA), dosed by individual mass flow controllers (UNIT Celarity). Water was dosed by an ISCO 100DM syringe pump through a heated capillary. Mixtures of NO and  $\text{NO}_2$  were obtained by feeding NO and oxygen through a long capillary, giving  $\text{NO}_x$  with 26–47%  $\text{NO}_2$ . Reaction products were analysed by a Thermo Fisher Nicolet 6700 FTIR analyser, equipped with a gas cell (2 m optical pathlength). Gas capillaries were heated to ~130 °C and the FTIR gas cell to 165 °C to avoid condensation of water and formation of ammonium nitrate. To simplify experimental procedure we are not using  $\text{CO}_2$  in the study as we have not observed  $\text{CO}_2$  effect on the  $\text{NO}_x$  SCR by  $\text{NH}_3$  during the preliminary experiments with  $\text{Ag}/\text{Al}_2\text{O}_3$  catalysts.

Conversions were calculated using the following equations:

$$X_{\text{NO}_x} = 1 - \frac{C_{\text{NO}_x}^{\text{outlet}}}{C_{\text{NO}_x}^{\text{inlet}}} \quad (1)$$

where  $X_{\text{NO}_x}$  denotes total conversion of  $\text{NO}_x$  and  $C_{\text{NO}_x}^{\text{inlet}}$  and  $C_{\text{NO}_x}^{\text{outlet}}$  is the  $\text{NO}_x$  concentrations on the inlet and outlet of the reactor, where:

$$C_{\text{NO}_x} = C_{\text{NO}} + C_{\text{NO}_2} \quad (2)$$

$\text{NH}_3$  conversion (total),  $\text{NH}_3$  conversion to  $\text{NO}_x$  (when no  $\text{NO}_x$  is fed) and NO conversion to  $\text{NO}_2$  (when no  $\text{NH}_3$  was fed) were calculated correspondingly:

$$X_{\text{NH}_3} = 1 - \frac{C_{\text{NH}_3}^{\text{outlet}}}{C_{\text{NH}_3}^{\text{inlet}}} \quad (3)$$

$$X_{\text{NH}_3 \rightarrow \text{NO}_x} = \frac{C_{\text{NO}_x}^{\text{outlet}}}{C_{\text{NH}_3}^{\text{inlet}}} \quad (4)$$

$$X_{\text{NO} \rightarrow \text{NO}_2} = \frac{C_{\text{NO}_2}^{\text{outlet}}}{C_{\text{NO}}^{\text{inlet}}} \quad (5)$$

and the ratio of converted NO to converted  $\text{NO}_2$  in the experiments with NO and  $\text{NO}_2$  mixtures:

$$\frac{C_{\text{NO}}^{\text{conv.}}}{C_{\text{NO}_2}^{\text{conv.}}} = \frac{C_{\text{NO}}^{\text{inlet}} - C_{\text{NO}}^{\text{outlet}}}{C_{\text{NO}_2}^{\text{inlet}} - C_{\text{NO}_2}^{\text{outlet}}} \quad (6)$$

$\text{NH}_3:\text{NO}_x$  conversion ratio below 400 °C was always 1:0.95–1.05 for all tested catalysts, therefore we are presenting only  $\text{NO}_x$  conversion values in the discussion.

### 2.4. DRIFTS studies

In-situ diffuse reflectance infrared Fourier transform spectroscopy (DRIFTS) experiments were performed using a BioRad FTS 6000 FTIR spectrometer equipped with a high-temperature reaction cell (Harrick Scientific, Praying Mantis) with KBr windows. The temperature of the reaction cell was controlled with a K-type thermocouple connected to a Eurotherm 2416 temperature controller. Gases were introduced into the reaction cell via individual mass flow controllers (Bronkhorst Hi-Tech). The gas composition at the outlet of the DRIFTS cell was analysed by a mass spectrometer (Balzers QuadStar 420).

Each experiment was performed using approximately 100 mg of  $\text{Ag}/\text{Al}_2\text{O}_3$  powder, using new powder for each experiment. The powder was initially pretreated in a flow of 8%  $\text{O}_2$  in Ar at 500 °C for 30 min, subsequently a background spectrum (60 scans, resolution 2  $\text{cm}^{-1}$  at 4000  $\text{cm}^{-1}$ ) was recorded in a flow of Ar. At 500 °C, 185 ppm  $\text{NO}_2$ , 315 ppm NO, 520 ppm  $\text{NH}_3$  and 8.3%  $\text{O}_2$  were added to the feed. Then the catalyst was cooled with a ramp rate of 10 °C/min in the reaction mixture to reaction temperature, where

the temperature is held for 10 min for stabilisation. Subsequently, NH<sub>3</sub> is removed from the feed gas mixture for 30 min and added again to it for 10 min. This procedure was repeated once. Thereafter, 1250 ppm H<sub>2</sub> were added for 10 min to the feed gas and, subsequently, NH<sub>3</sub> was removed again. The evolution of absorption bands in the spectra was followed using the kinetic mode (9 scans/spectrum, 6 spectra/min,) at a resolution of 2 cm<sup>-1</sup> at 4000 cm<sup>-1</sup>. The data are presented as absorbance, which is defined as the logarithm of the inverse reflectance (log 1/R). All DRIFTS experiments were carried out using a total flow rate of 100 ml/min which corresponds to a space velocity of about 62,000 h<sup>-1</sup>.

## 2.5. DFT calculations

Plane wave DFT code DACAPO is used to calculate the adsorption energies and the gas phase energies of the adsorbates. Plane wave cutoff of 340.15 eV and density cutoff of 680 eV are used for the calculations. The core electrons are described by the Vanderbilt ultrasoft pseudopotential [22]. RBPE is used as the exchange correlation energy function [23]. Fermi population of the Kohn-Sham states is  $k_b T = 0.1$  eV. The convergence limit is set as maximum change in force constant  $f_{\max} = 0.03$  eV.

The adsorption energies of O, NO, NO<sub>2</sub> and NO<sub>3</sub> are studied over six different transition metals (Ag, Cu, Pd, Pt, Rh, Ru) on both the (111) terrace and the (211) step surfaces. We use a 2 × 2 surface cell for O and NO for (111) terrace, 2 × 1 surface cell for O and NO for (211) step surface, 3 × 3 surface cell for NO<sub>2</sub> and NO<sub>3</sub> adsorption study on (111) terrace and the 3 × 1 surface cell for NO<sub>2</sub> and NO<sub>3</sub> adsorption study (211) step surfaces, with 8 × 8 × 1 Monkhorst-Pack **k**-point sampling in the irreducible Brillouin zone for all the 2 × 2 surface cells, 8 × 6 × 1 Monkhorst-Pack **k**-point sampling in the irreducible Brillouin zone for all the 2 × 1 surface cells and 4 × 4 × 1 Monkhorst-Pack **k**-point sampling for both 3 × 3 and 3 × 1 surface cells. For all the (111) surfaces we use a four-layer slab where the two topmost layers are allowed to relax whereas for the (211) surfaces with 2 × 1 surface cell we use a slab model with twelve layers where the topmost six layers are allowed to relax and for (211) surfaces with 3 × 1 surface cell we use a slab model with nine layers where the topmost three layers are allowed to relax.

For the calculation of γ-Al<sub>2</sub>O<sub>3</sub> and the adsorption of different species on γ-Al<sub>2</sub>O<sub>3</sub> we also used the DACAPO code with a plane wave cutoff of 340.15 eV and a density cutoff of 680 eV. A 4 × 4 × 1 Monkhorst-Pack **k**-point sampling in the irreducible Brillouin zone was used for γ-Al<sub>2</sub>O<sub>3</sub>. The γ-Al<sub>2</sub>O<sub>3</sub> surface was modelled by a step on a nonspinel γ-Al<sub>2</sub>O<sub>3</sub> structure which was derived bulk γ-Al<sub>2</sub>O<sub>3</sub> model [24]. The cell parameters for the γ-Al<sub>2</sub>O<sub>3</sub> step closed packed surface are  $a = 8.0680$  Å and  $b = 10.0092$  Å and  $\alpha = \beta = \gamma = 90^\circ$ . For the γ-Al<sub>2</sub>O<sub>3</sub> surface the bottom two layers were fixed whereas the top three layers were allowed to relax.

In all the model surfaces, the neighboring slabs are separated by more than 10 Å of vacuum.

NO<sub>x</sub> and HNO<sub>x</sub> adsorption energies were calculated relative to gas phase zero energy points of these species.

The energy minimum adsorption geometries used in the calculations are presented in the supplementary material.

## 3. Results and discussion

### 3.1. Unique activity of Ag/Al<sub>2</sub>O<sub>3</sub> in H<sub>2</sub>-assisted NH<sub>3</sub>-deNO<sub>x</sub>

NO<sub>x</sub> conversions obtained over the prepared catalysts at 380 °C tested under the conditions of SCR of NO<sub>x</sub> with NH<sub>3</sub>, without and with H<sub>2</sub> in the exhaust, are given in Table 1. In the absence of H<sub>2</sub> all the catalysts are inert with respect to NO<sub>x</sub> reduction or ammonia

**Table 1**

Studied catalysts and NO<sub>x</sub> conversions obtained at 380 °C without and with H<sub>2</sub> in the feed gas. Reaction conditions: 500 ppm NO, 520 ppm NH<sub>3</sub>, 8.3% O<sub>2</sub>, 7% H<sub>2</sub>O in Ar, GHSV = 110,000 h<sup>-1</sup>.

Catalyst	Metal loading, wt%	Support BET surface area, m <sup>2</sup> /g	NO <sub>x</sub> conversion	
			0 ppm H <sub>2</sub>	1200 ppm H <sub>2</sub>
Al <sub>2</sub> O <sub>3</sub>	–	140	0	0
Ag/Al <sub>2</sub> O <sub>3</sub>	1	140	0	94
Ag/TiO <sub>2</sub>	1	110	1.5	25
Ag/ZrO <sub>2</sub>	1	14	0	0
Sn/Al <sub>2</sub> O <sub>3</sub>	3	140	0	0
In/Al <sub>2</sub> O <sub>3</sub>	3	140	0	10.5

oxidation at temperatures below 400 °C. The hydrogen effect was observed only for Ag/Al<sub>2</sub>O<sub>3</sub>, Ag/TiO<sub>2</sub> and In/Al<sub>2</sub>O<sub>3</sub> (Fig. 1). The former catalyst demonstrates extremely high performance with NO<sub>x</sub> conversion exceeding 80% at 200 °C at GHSV = 110,000 h<sup>-1</sup>. No more than 5 ppm N<sub>2</sub>O was observed in the products. Ag/TiO<sub>2</sub> is much less active with maximum NO<sub>x</sub> conversion of 25% at 380 °C. The activity of In/Al<sub>2</sub>O<sub>3</sub> below 400 °C is only marginal. Therefore only Ag/Al<sub>2</sub>O<sub>3</sub> may be considered for practical applications among the tested catalysts. Furthermore, it is evident that both silver and alumina are necessary components of the catalyst to obtain a high performance in deNO<sub>x</sub>. Removal or change of each of these components lead to almost inactive catalysts. Therefore, it is likely that both silver and alumina take part in the catalytic cycle or the active site is positioned on the interface between Ag and Al<sub>2</sub>O<sub>3</sub>.

#### 3.1.1. TEM data on Ag/Al<sub>2</sub>O<sub>3</sub> and Ag/TiO<sub>2</sub>

In order to clarify if it is the catalyst morphology that determines the drastic difference in the SCR performance of Ag/Al<sub>2</sub>O<sub>3</sub> and Ag/TiO<sub>2</sub>, TEM images of the samples were obtained. These micrographs are compared in Fig. 2. The choice of the catalysts in question is dictated by their common properties (Ag loading, BET surface area of the support, preparation technique), which is in contrast to their very different catalytic activity.

EDX shows the presence of ~1% Ag in the both depicted catalyst grains. However, we were unable to locate any metal particles with diameters larger than 2–3 nm in both catalyst samples. This confirms a high dispersion of Ag in both Ag/Al<sub>2</sub>O<sub>3</sub> and Ag/TiO<sub>2</sub>.

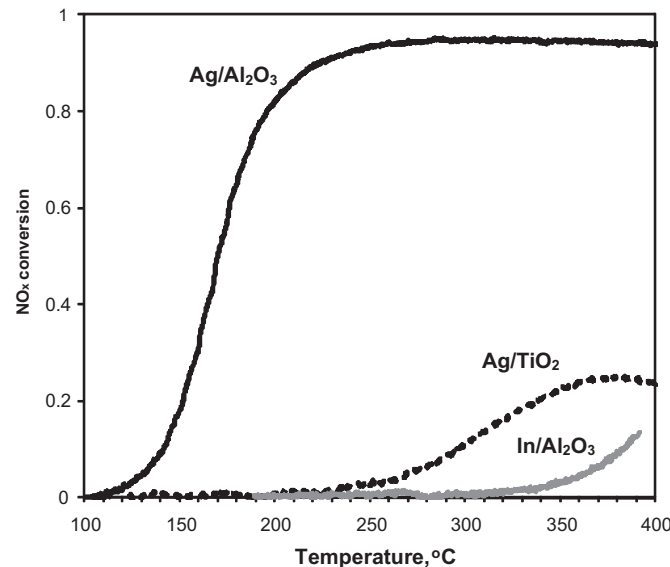


**Fig. 1.** NO<sub>x</sub> conversion profiles obtained over Ag/Al<sub>2</sub>O<sub>3</sub>, Ag/TiO<sub>2</sub>, and In/Al<sub>2</sub>O<sub>3</sub>. Reaction conditions: 500 ppm NO, 520 ppm NH<sub>3</sub>, 1200 ppm H<sub>2</sub>, 8.3% O<sub>2</sub>, 7% H<sub>2</sub>O in Ar, GHSV = 110,000 h<sup>-1</sup>.

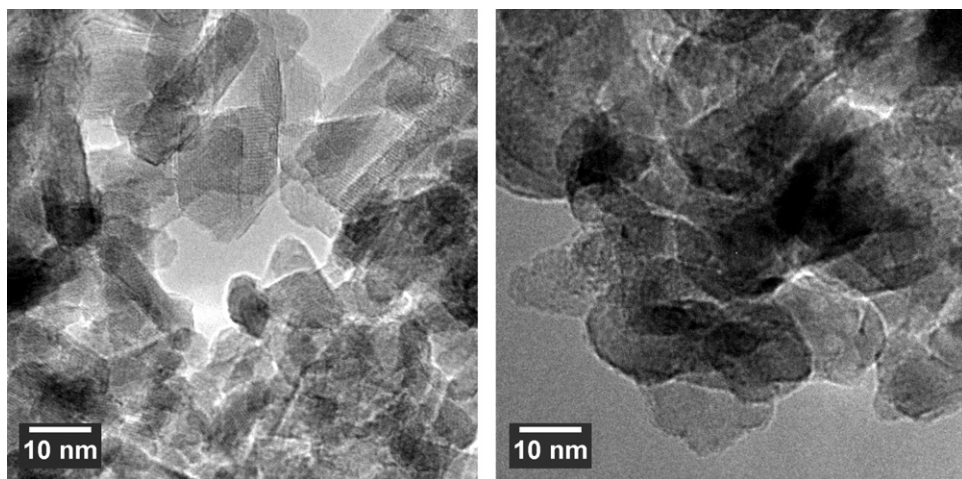


**Fig. 2.** TEM images of Ag/Al<sub>2</sub>O<sub>3</sub> (left) and Ag/TiO<sub>2</sub> (right) calcined at 550 °C in air.

catalysts, which might be in the form of clusters of 4–8 Ag atoms as suggested by Kondratenko et al. [16]. Therefore the large difference in SCR activity of Ag/Al<sub>2</sub>O<sub>3</sub> and Ag/TiO<sub>2</sub> is not due to a large difference in Ag dispersion.

### 3.2. Study of the mechanism of H<sub>2</sub>-assisted NH<sub>3</sub>-deNO<sub>x</sub>

#### 3.2.1. Experiments with Ag/Al<sub>2</sub>O<sub>3</sub> where components of the feed are omitted

Studies of the mechanism of hydrogen-assisted NO<sub>x</sub> SCR by NH<sub>3</sub> on Ag/Al<sub>2</sub>O<sub>3</sub> were already performed before [16,17], where the attention was drawn to the state of silver. Our catalytic experiments show a uniqueness of the Ag/Al<sub>2</sub>O<sub>3</sub> catalytic system, in which both components play a vital role.

To have a notion of the individual reactions occurring during NO<sub>x</sub> SCR by NH<sub>3</sub> we consecutively run catalytic tests with one of the components absent in the feed.

According to the results obtained so far it is already clear that the removal of hydrogen leads to a completely inactive catalyst with regards to NH<sub>3</sub>-deNO<sub>x</sub> (Table 1) or ammonia oxidation. The concentration of all monitored gases remained constant during temperature ramping from 400 to 100 °C when no H<sub>2</sub> was in the feed. The same is true for the removal of oxygen from the feed – no NO reduction or NH<sub>3</sub> oxidation was observed without O<sub>2</sub>.

When NH<sub>3</sub> was removed from the gas feed, a pronounced oxidation of NO to NO<sub>2</sub> starting from 100 °C was observed (Fig. 3, solid line). Together with that a very low NO<sub>x</sub> to N<sub>2</sub> conversion (dotted line, max. 4%) was observed indicating that hydrogen normally acts not as the main reductant but as a co-reductant. When both ammonia and hydrogen were removed from the feed, no oxidation of NO to NO<sub>2</sub> was observed.

The latter observation agrees with the data obtained in [6,16]. As suggested in [6], hydrogen addition promotes oxidation of NO. However, we observed no oxidation of NO to NO<sub>2</sub> during the experiments with Ag/TiO<sub>2</sub> and Ag/ZrO<sub>2</sub> catalysts. This shows once again that not only Ag, but also the support plays an important role in the catalytic activity of Ag/Al<sub>2</sub>O<sub>3</sub> which also agrees with the data on C<sub>3</sub>H<sub>8</sub>-SCR reported in [6].

The mechanism of O<sub>2</sub> activation by hydrogen has been suggested earlier [25,26] as follows. On the first step hydrogen dissociates on active Ag<sub>n</sub><sup>+</sup> sites on alumina to form an acidic proton and hydride Ag<sub>n</sub>-H. This hydride later reacts with oxygen to form a reactive oxidant, such as hydroperoxy radicals (HO<sub>2</sub>), peroxide (O<sub>2</sub><sup>2-</sup>), or superoxide ions (O<sub>2</sub><sup>-</sup>) all of which later oxidise NO to NO<sub>2</sub>.

When removing NO from the NO, NH<sub>3</sub>, H<sub>2</sub>, O<sub>2</sub> and H<sub>2</sub>O containing feed, NH<sub>3</sub> oxidation to N<sub>2</sub> (Fig. 4, solid line) and to NO<sub>x</sub> (Fig. 4, dotted line) occurs at temperatures higher than 200 °C. Comparison of the data in Fig. 3 and Fig. 4 suggests that NO oxidative activation starts at significantly lower temperature (corresponding to the NH<sub>3</sub>-deNO<sub>x</sub> light-off temperature) than NH<sub>3</sub> oxidative activation. Therefore it is more likely that oxidative activation of NO is an important step in the overall catalytic mechanism of NO<sub>x</sub> SCR over Ag/Al<sub>2</sub>O<sub>3</sub>.

The data does not support a hypothesis of oxidative dehydrogenation of NH<sub>3</sub> (or NH<sub>3</sub>-assisted NO decomposition) being the main catalysed step of H<sub>2</sub>-assisted NH<sub>3</sub>-deNO<sub>x</sub> over Ag/Al<sub>2</sub>O<sub>3</sub> [18]. Ag/Al<sub>2</sub>O<sub>3</sub> rather participates in NO activation and possibly in the reaction of NH<sub>3</sub> with NO<sub>x</sub> intermediates [16].

The hydrogen promoted oxidative activation of NO has been already reported by Satokawa et al. for NO<sub>x</sub> SCR by C<sub>3</sub>H<sub>8</sub> [6]. However in that study oxidative activation of NO was not enough to initiate SCR and activation of C<sub>3</sub>H<sub>8</sub> by H<sub>2</sub> has been reported to be necessary which makes it different from SCR by NH<sub>3</sub>.

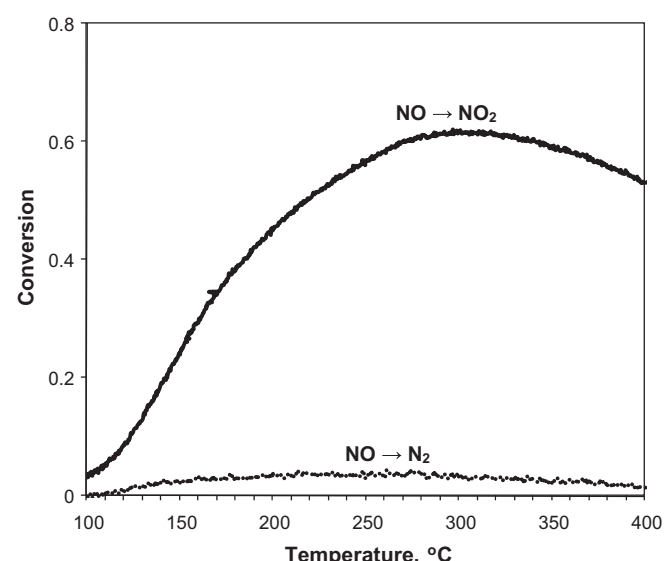


**Fig. 3.** NO conversion to NO<sub>2</sub> (solid line) and NO<sub>x</sub> conversion to N<sub>2</sub> (dotted line) over Ag/Al<sub>2</sub>O<sub>3</sub> without ammonia in the feed. Reaction conditions: 500 ppm NO, 1200 ppm H<sub>2</sub>, 8.3% O<sub>2</sub>, 7% H<sub>2</sub>O in Ar, GHSV = 110,000 h<sup>-1</sup>.

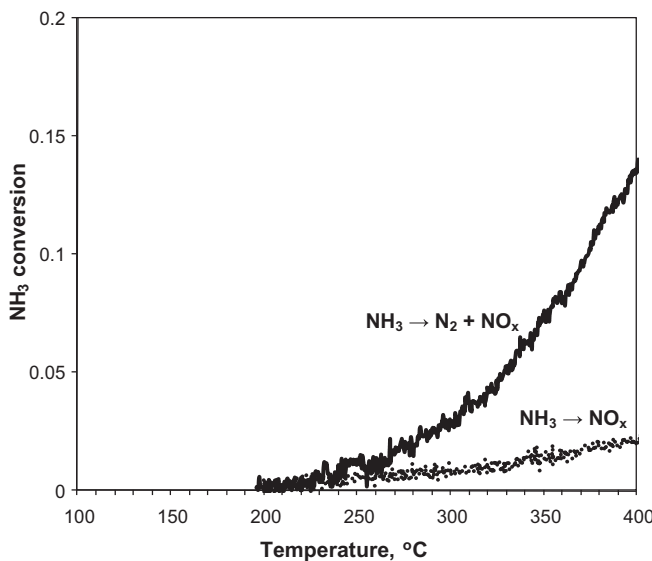


**Fig. 4.** Total  $\text{NH}_3$  conversion (solid line) and  $\text{NH}_3$  conversion to  $\text{NO}_x$  (dotted line) over  $\text{Ag}/\text{Al}_2\text{O}_3$  with no  $\text{NO}$  in the feed. Reaction conditions: 520 ppm  $\text{NH}_3$ , 1200 ppm  $\text{H}_2$ , 8.3%  $\text{O}_2$ , 7%  $\text{H}_2\text{O}$  in Ar,  $\text{GHSV} = 110,000 \text{ h}^{-1}$ .

### 3.2.2. Experiments with feeding $\text{NO}$ and $\text{NO}_2$ mixtures over $\text{Ag}/\text{Al}_2\text{O}_3$ and $\text{Ag}/\text{ZrO}_2$

After realizing that the hydrogen promoted oxidation of  $\text{NO}$  to  $\text{NO}_2$  may be the first step in the  $\text{H}_2$ -assisted  $\text{NH}_3$ -de $\text{NO}_x$  we decided to do catalytic tests with a feed containing a mixture of  $\text{NO}$  and  $\text{NO}_2$  as  $\text{NO}_x$ . Since  $\text{H}_2$  facilitates reversible  $\text{NO}-\text{NO}_2$  transformation, undesirable for these experiments, no  $\text{H}_2$  was co-fed.

Fig. 5 shows  $\text{NO}_x$  conversions to  $\text{N}_2$  obtained over  $\text{Ag}/\text{Al}_2\text{O}_3$  when a  $\text{NO}$  and  $\text{NO}_2$  mixture is fed as  $\text{NO}_x$  (containing 26, 34 and 47%  $\text{NO}_2$ ) and over  $\text{Ag}/\text{ZrO}_2$  with 34%  $\text{NO}_2$  in  $\text{NO}$  as  $\text{NO}_x$ . Surprisingly for all three cases we observe nearly equal, maximum 30%,  $\text{NO}_x$  conversion which changes only slightly with temperature.  $\text{NH}_3$  conversion profiles follow the  $\text{NO}_x$  conversion profiles and they are therefore not shown. This observation allows us to conclude that oxidation of  $\text{NO}$  to  $\text{NO}_2$  over  $\text{Ag}/\text{Al}_2\text{O}_3$ , at least, partially accounts

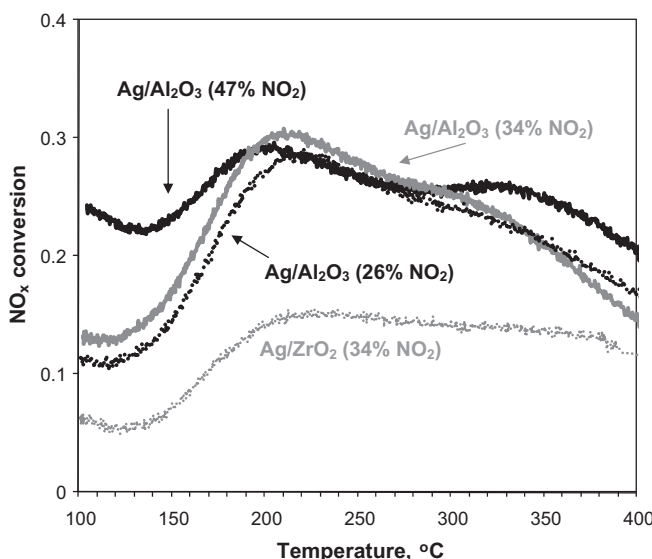


**Fig. 5.**  $\text{NO}_x$  conversion over  $\text{Ag}/\text{Al}_2\text{O}_3$  and  $\text{Ag}/\text{ZrO}_2$  without  $\text{H}_2$  in the feed, when  $\text{NO}$  and  $\text{NO}_2$  mixture is fed as  $\text{NO}_x$  ( $\text{NO}_2$  content is specified,  $\text{NO}$  is the rest of 500 ppm  $\text{NO}_x$ ). Conditions: 500 ppm  $\text{NO}_x$ , 520 ppm  $\text{NH}_3$ , 8.3%  $\text{O}_2$ , 7%  $\text{H}_2\text{O}$  in Ar,  $\text{GHSV} = 110,000 \text{ h}^{-1}$ .

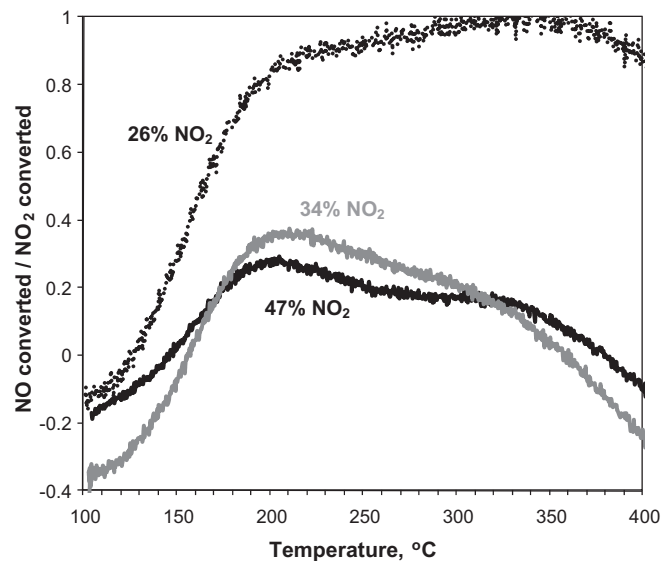


**Fig. 6.** Ratio of consumed  $\text{NO}$  to consumed  $\text{NO}_2$  for simultaneous  $\text{NO}+\text{NO}_2$  reduction by  $\text{NH}_3$  over  $\text{Ag}/\text{Al}_2\text{O}_3$ . Reaction conditions: 500 ppm  $\text{NO}_x$  ( $\text{NO}_2$  fraction is stated near the corresponding curves), 520 ppm  $\text{NH}_3$ , 8.3%  $\text{O}_2$ , 7%  $\text{H}_2\text{O}$  in Ar,  $\text{GHSV} = 110,000 \text{ h}^{-1}$ .

for the activity of this catalyst in the  $\text{NO}_x$  SCR. This agrees with previous works, evidencing oxidation of  $\text{NO}$  to  $\text{NO}_2$  involving  $\text{H}_2$  [25] and supposing it to be crucial for low-temperature  $\text{NO}_x$  SCR by hydrocarbons [27].

Moreover, SCR of the  $\text{NO}$  and  $\text{NO}_2$  mixture by  $\text{NH}_3$  is not a unique feature of  $\text{Ag}/\text{Al}_2\text{O}_3$  but was also observed for other supports though to a less extent, e.g. with 15% maximum  $\text{NO}_x$  conversion in the case of  $\text{Ag}/\text{ZrO}_2$  (see Fig. 5, gray dotted line). Thus, metal oxides other than alumina can catalyse  $\text{NO}+\text{NO}_2$  SCR by  $\text{NH}_3$  but  $\text{Ag}/\text{Al}_2\text{O}_3$  with  $\text{H}_2$  co-feeding is required to oxidise  $\text{NO}$  at low temperatures. Therefore, we are focusing our study on  $\text{Ag}/\text{Al}_2\text{O}_3$  catalysts and the corresponding alumina support.

The effect of increasing the  $\text{NO}_x$  SCR rate by feeding  $\text{NO}$  and  $\text{NO}_2$  mixture has already been noticed for other catalytic systems including vanadia-based catalysts [28] and zeolites [29]. The effect is called “Fast-SCR” and characterised by a well-defined stoichiometry of  $\text{NO}:\text{NO}_2$  being 1:1.

To check if the  $\text{NO}:\text{NO}_2$  conversion without  $\text{H}_2$  in the feed can be ascribed to “Fast SCR” [29], we calculated the ratio of consumed  $\text{NO}$  to consumed  $\text{NO}_2$  (Fig. 6). In our case the ratio of consumed  $\text{NO}$  to consumed  $\text{NO}_2$  changed with temperature from negative values (only  $\text{NO}_2$  is consumed and a small amount of  $\text{NO}$  is produced from it) to positive values up to 1 in case of feeding 26%  $\text{NO}_2$  (Fig. 6). Interestingly, the temperature at which  $\text{NO}$  starts to be consumed ( $\sim 150^\circ\text{C}$ ) coincides with the onset temperature of  $\text{H}_2$ -assisted SCR (Fig. 1). Therefore, we can suppose that parts of the mechanisms of both  $\text{H}_2$ -assisted  $\text{NO}$  SCR by  $\text{NH}_3$  and  $\text{NO}+\text{NO}_2$  SCR by  $\text{NH}_3$  are similar. But in case of  $\text{NO}+\text{NO}_2$  SCR we observed a conversion limit at  $\sim 30\%$ , when almost 100% conversion is obtained in  $\text{H}_2$ -assisted  $\text{NO}_x$ -SCR. This could be explained by blocking of the catalyst surface by adsorbed nitrate species [25]. The poisoning effect of surface nitrates for propane-SCR was observed in [26], where the authors also demonstrated the ability of hydrogen to effectively remove adsorbed nitrate species. Thus, introduction of hydrogen may facilitate not only  $\text{NO}$  to  $\text{NO}_2$  conversion, but also regeneration of the catalyst surface, which removes the 30% conversion limit.

In general, the ratio of converted  $\text{NO}$  to converted  $\text{NO}_2$  depends on the total amount of  $\text{NO}_2$  in the feed and decreases with increase in  $\text{NO}_2$  content. The higher the  $\text{NO}_2$  content – the larger is the part of  $\text{NO}_2$  in the  $\text{NO}_x$  that is converted to  $\text{N}_2$ . Independent on this,

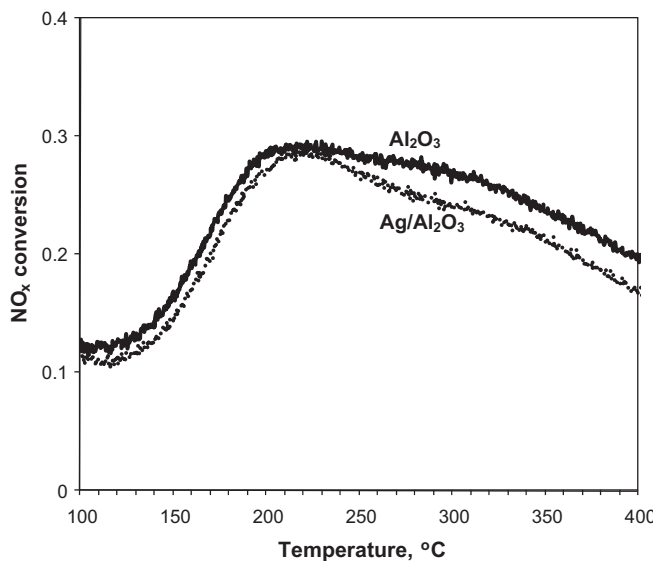


**Fig. 7.** NO<sub>x</sub> conversion over Al<sub>2</sub>O<sub>3</sub> (solid line) and Ag/Al<sub>2</sub>O<sub>3</sub> (dotted line, for a comparison) without H<sub>2</sub> in the feed, when NO and NO<sub>2</sub> mixture is fed as NO<sub>x</sub>. Reaction conditions: 500 ppm NO<sub>x</sub> (37% NO<sub>2</sub>), 520 ppm NH<sub>3</sub>, 8.3% O<sub>2</sub>, 7% H<sub>2</sub>O in Ar, GHSV = 110,000 h<sup>-1</sup>.

the ratio of converted NO<sub>x</sub> to converted NH<sub>3</sub> was always 1:1 and maximum conversion remained constant at ~30%.

### 3.2.3. Experiments with feeding NO and NO<sub>2</sub> mixtures over pure γ-Al<sub>2</sub>O<sub>3</sub>

In some of the papers on H<sub>2</sub>-assisted NO SCR by NH<sub>3</sub>, published earlier [16,17], alumina was considered only as a support for the active Ag nanoparticles. In this case, the properties of alumina could influence the catalyst activity indirectly by tuning the Ag particle size and distribution. In the following we test this assumption.

With or without hydrogen γ-alumina stays inactive under the experimental conditions of NO<sub>x</sub> SCR by ammonia when NO is the only component of NO<sub>x</sub> in the feed. This changes when NO<sub>2</sub> is introduced. Fig. 7 shows a comparison of NO<sub>x</sub> (26% NO<sub>2</sub> of total NO<sub>x</sub> at the reactor inlet) conversion by NH<sub>3</sub> obtained over pure Al<sub>2</sub>O<sub>3</sub> (solid line) and Ag/Al<sub>2</sub>O<sub>3</sub> (dotted line) with no H<sub>2</sub> in the feed. The profiles are almost identical indicating that presence of Ag in the catalyst is important only for the H<sub>2</sub>-assisted reaction. Taking into account the overall quantity of NO<sub>2</sub>, which can be produced from NO in presence of H<sub>2</sub> over Ag/Al<sub>2</sub>O<sub>3</sub> (Fig. 3), it is evident that alumina can significantly contribute to the overall H<sub>2</sub>-assisted NO SCR mechanism. Thus, it cannot be neglected that alumina is an active part of the catalyst. Moreover the stoichiometry of NO + NO<sub>2</sub> SCR conversion over alumina follows the same trend as for the Ag/Al<sub>2</sub>O<sub>3</sub> (Fig. 8), which may demonstrate the same mechanism is working in both cases. Running NO + NO<sub>2</sub> SCR with H<sub>2</sub> in the feed over pure Al<sub>2</sub>O<sub>3</sub> yield almost the same NO<sub>x</sub> conversion as as for the test without H<sub>2</sub> (Fig. 7, solid line).

Thus, the presence of Ag and H<sub>2</sub> is mostly important for oxidative activation of NO and possibly removal of adsorbed species blocking the catalyst surface. The reaction of NO and NH<sub>3</sub> with the obtained NO<sub>2</sub> can proceed further over pure Al<sub>2</sub>O<sub>3</sub> yielding N<sub>2</sub>. This result agrees with the results of Lee et al. [30], who demonstrated the ability of pure alumina to catalyse the reduction of NO, activated over Ag/Al<sub>2</sub>O<sub>3</sub>, by partially oxidised hydrocarbons. At the same time, Meunier and Ross [31] observed the ability of pure alumina to run the propene SCR of NO<sub>2</sub> (but not of NO).

From the analysis of the stoichiometry of the NO + NO<sub>2</sub> SCR reaction (Figs. 6 and 8) it can be concluded that at temperatures lower than 150 °C only NO<sub>2</sub> reacts with NH<sub>3</sub>. The production of NO from

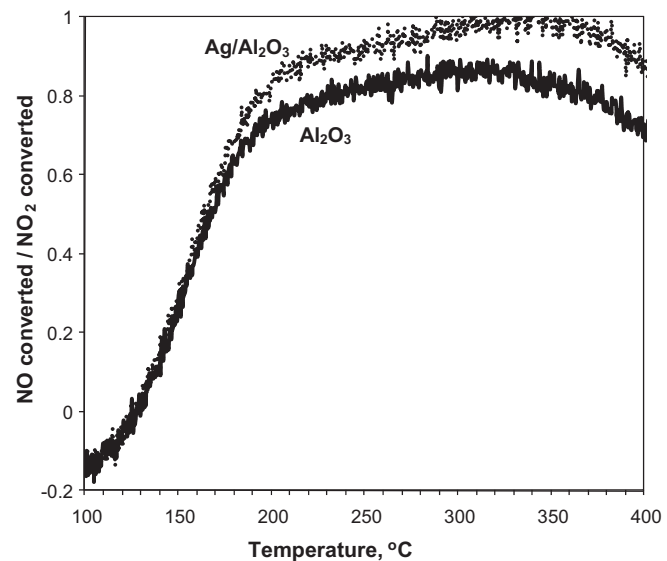
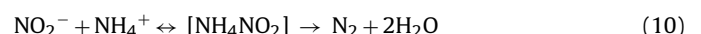
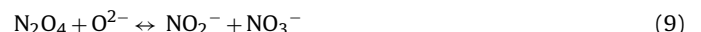


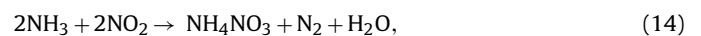
**Fig. 8.** Ratio of consumed NO to consumed NO<sub>2</sub> for NO + NO<sub>2</sub> simultaneous reduction by NH<sub>3</sub> over Al<sub>2</sub>O<sub>3</sub> (solid line) and Ag/Al<sub>2</sub>O<sub>3</sub> (dotted line, for a comparison). Reaction conditions: 500 ppm NO<sub>x</sub> (26% NO<sub>2</sub>), 520 ppm NH<sub>3</sub>, 8.3% O<sub>2</sub>, 7% H<sub>2</sub>O in Ar, GHSV = 110,000 h<sup>-1</sup>.

NO<sub>2</sub> can also be observed, which is thermodynamically not possible and is likely due to an uncomplete SCR reaction between NO<sub>2</sub> and NH<sub>3</sub>. Above 350 °C NO<sub>2</sub> decomposition to NO is thermodynamically favorable, and this may be a reason of decreasing apparent amount of consumed NO [32]. Only between 150 and 350 °C NO consumption is significant and almost equal to NO<sub>2</sub> consumption in the case of 26% NO<sub>2</sub> in NO<sub>x</sub> feed. Based on the knowledge of the “Fast SCR” [29] the following reactions can be proposed:



According to the scheme, at temperatures higher than 150 °C reactions (7)–(11) take place yielding nitrogen and surface nitrate species. Disproportionation of adsorbed NO<sub>2</sub> (8), (9) was also suggested by DFT calculations earlier [33]. A small part of the surface nitrates is decomposed to N<sub>2</sub>O (12), trace amount of which (<5 ppm) is observed in the reaction products at high temperatures. NO production from NO<sub>2</sub> (negative NO<sub>converted</sub>/NO<sub>2converted</sub> ratio at T < 150 °C on Fig. 6) and the observation that the higher the NO<sub>2</sub> content – the larger is the part of NO<sub>2</sub> in the NO<sub>x</sub> that is converted to N<sub>2</sub> in the NO/NO<sub>2</sub> experiments can be explained by reverse (13). NO reacts with surface nitrates according to (13) to form NO<sub>2</sub> and nitrite, which is readily decomposed to nitrogen (10). With that nitrates are partly removed from the catalyst surface and higher NO<sub>x</sub> conversion is obtained.

With decreasing reaction temperature from 400 to 200 °C an increase in the NO<sub>x</sub> conversion is observed. The effect is particularly evident for the 47% NO<sub>2</sub> + NO mixture (Fig. 5, solid curve) and may be due to the formation of surface NH<sub>4</sub>NO<sub>3</sub>. NH<sub>4</sub>NO<sub>3</sub> formation is also consistent with decreased NO<sub>converted</sub>/NO<sub>2converted</sub> ratio below 180 °C (Fig. 8) due to reaction stoichiometry:



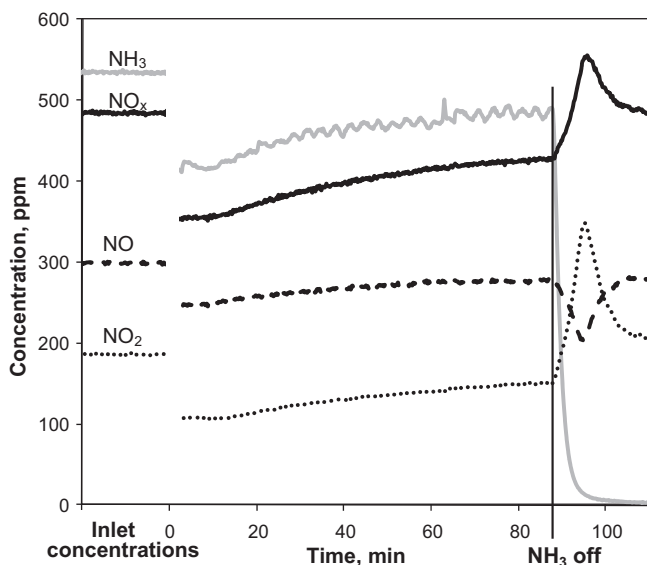


**Fig. 9.** Change of NO, NO<sub>2</sub> and NO<sub>x</sub> concentrations after removing NH<sub>3</sub> from the feed. Catalyst: Al<sub>2</sub>O<sub>3</sub>. Reaction conditions: 500 ppm NO<sub>x</sub> (37% NO<sub>2</sub>), 520 ppm NH<sub>3</sub>, 8.3% O<sub>2</sub>, 7% H<sub>2</sub>O in Ar, GHSV = 110,000 h<sup>-1</sup>, temperature 210 °C.

which is, in fact, a combination of (7)+(8)+(9)+(10)+(11), but without (12) and (13), which are too slow at this temperature. It is also rather indicative of NH<sub>4</sub>NO<sub>3</sub> formation that below 200 °C we do not observe N<sub>2</sub>O evolution, while above this temperature its decomposition (12) yields N<sub>2</sub>O. Therefore, below 200 °C nitrate formation and subsequent blocking the alumina surface limits NO<sub>x</sub> conversion.

To check the reaction scheme during an Al<sub>2</sub>O<sub>3</sub> activity test, temperature ramping was stopped at 500, 210 and 100 °C. After the concentrations of the outlet gas components were stabilised, NH<sub>3</sub> was switched off from the feed. Following the removal of NH<sub>3</sub> from the inlet gas at 500 and 100 °C the concentrations of NO and NO<sub>2</sub> equalled these concentrations at the reactor inlet (no reaction with adsorbed nitrates (13) was observed). However, the removal of NH<sub>3</sub> from the feed at 210 °C (Fig. 9) resulted in consumption of NO and release of NO<sub>2</sub>. This is in agreement with NO consumption in the NO<sub>x</sub> SCR over alumina, which takes place between 150 and 350 °C (Fig. 8). The ratio of evolved NO<sub>2</sub> to consumed NO was approximately 1.7. This ratio can be achieved by combination of the competing reactions (10), which gives no NO<sub>2</sub>, reverse (9) and (8), which give 2 NO<sub>2</sub> molecules, and, of course (13), which initiates the NO consumption and yields 1 NO<sub>2</sub> molecule. Thus the mechanism of NO<sub>x</sub> SCR by NH<sub>3</sub> over Al<sub>2</sub>O<sub>3</sub> and Ag/Al<sub>2</sub>O<sub>3</sub> could share most of the reaction steps with "Fast SCR".

### 3.2.4. Surface species during NH<sub>3</sub>-SCR over Al<sub>2</sub>O<sub>3</sub>

Diffuse reflectance infrared spectroscopy is a powerful tool to complement observations from catalytic experiments with observations of surface species. Fig. 10 shows the evolution of species on the Al<sub>2</sub>O<sub>3</sub> surface, when switching off NH<sub>3</sub> from a feed containing NO, NO<sub>2</sub>, NH<sub>3</sub> and O<sub>2</sub> at 150 °C and at 500 °C. Similar spectra were observed at 300 and 400 °C but not shown. The first spectra are taken in a feed containing NH<sub>3</sub> and the following spectra 5, 10, 15 and 25 min after the NH<sub>3</sub> was switched off. When all gases are present in the first spectra, bands at 1690, 1623, 1533, 1474, 1398, 1314 and 1236 cm<sup>-1</sup> can be distinguished at 150 °C. According to literature, the bands at 1623, 1533 and 1236 cm<sup>-1</sup> which are accompanied by bands at 3355, 3271 and 3173 cm<sup>-1</sup> (not shown) can be assigned to deformation vibrations and stretching vibrations of ammonia, respectively [34–37]. Bands at 1690 and 1474 cm<sup>-1</sup> have previously been assigned to deformation vibrations of NH<sub>4</sub><sup>+</sup>

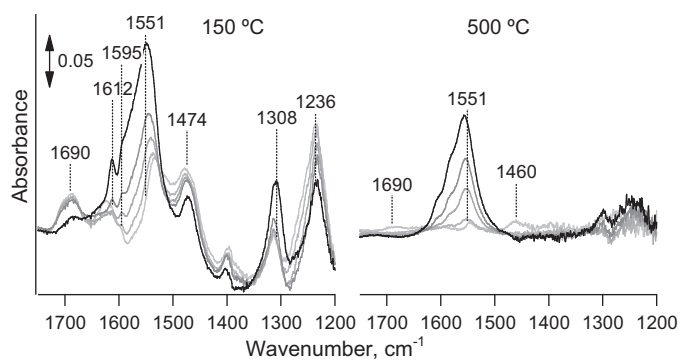


**Fig. 10.** Change in surface species after removing NH<sub>3</sub> for the first time from the feed over a fresh Al<sub>2</sub>O<sub>3</sub> catalyst. Reaction conditions: 500 ppm NO<sub>x</sub> (37% NO<sub>2</sub>), 520 ppm NH<sub>3</sub>, 8.3% O<sub>2</sub> in Ar. Spectra were taken from gray to black: with NH<sub>3</sub> in the feed, and 5, 10, 15 and 25 min after switching off NH<sub>3</sub>.

or NH<sub>3</sub> [34,35,37]. At 500 °C all the bands are much smaller. But even there, mainly bands due to NH<sub>3</sub> or NH<sub>4</sub><sup>+</sup> can be observed. Thus under NH<sub>3</sub>-SCR conditions, mainly ammonia is adsorbed on Al<sub>2</sub>O<sub>3</sub> and very little nitrates and nitrites are adsorbed. When turning off ammonia in the feed first the bands of adsorbed NH<sub>3</sub> at 1236, 1623, 3355, 3271 and 3173 cm<sup>-1</sup> decrease at 150 °C. Somewhat later, the NH<sub>4</sub><sup>+</sup> bands at 1690 and 1474 cm<sup>-1</sup> start to decrease and two new bands at 1612 and 1585 cm<sup>-1</sup> grow. At the same time, the bands around 1551 and 1308 cm<sup>-1</sup> shift in wavenumber and increase. The shifts in wavenumber as well as the new bands are all caused by the stretching of the N=O bond of differently bound nitrate species [35–45] which start accumulating in the absence of NH<sub>3</sub>. That the bands of adsorbed NH<sub>3</sub> diminish before the bands of adsorbed NH<sub>4</sub><sup>+</sup> species start to decrease is in accordance with reaction (14). Switching back to SCR reaction conditions, the NH<sub>3</sub> and NH<sub>4</sub><sup>+</sup> species start growing again at 150 °C while the nitrate species decrease but do not completely disappear, even in the presence of H<sub>2</sub> as shown by the first spectra in Fig. 11.

At 500 °C, the bands of adsorbed NH<sub>4</sub><sup>+</sup> at 1690 and 1464 cm<sup>-1</sup> disappear previous to the bands of adsorbed NH<sub>3</sub> between 3355 and 3173 cm<sup>-1</sup> (not shown), while the nitrate band at about 1551 cm<sup>-1</sup> increases. The remaining nitrates may be regarded as inactive. However, whether the accumulation of these species reduce the

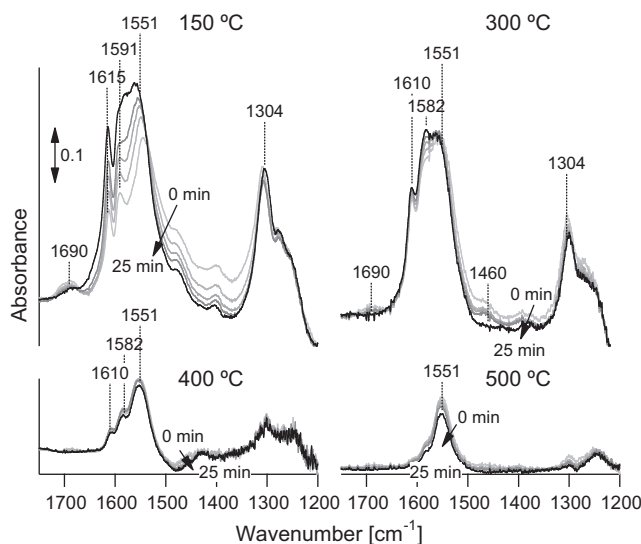


**Fig. 11.** Change in surface species after removing NH<sub>3</sub> from the hydrogen-containing feed over Al<sub>2</sub>O<sub>3</sub>. Reaction conditions: 500 ppm NO<sub>x</sub> (37% NO<sub>2</sub>), 520 ppm NH<sub>3</sub>, 1250 ppm H<sub>2</sub>, 8.3% O<sub>2</sub> in Ar. Spectra were taken from gray to black: with NH<sub>3</sub> in the feed, and 5, 10, 15 and 25 min after switching off NH<sub>3</sub>.

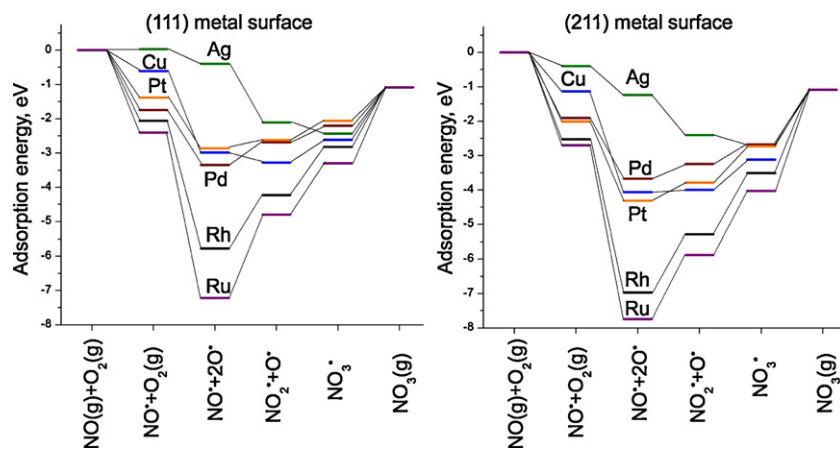


**Fig. 12.** Potential energy surface diagram for the formation of NO<sub>x</sub> via the oxidation of NO over (111) and (211) surfaces of the selected transition metals.

activity for NO<sub>x</sub> reduction and, thus, poison the surface or only act as spectator species, cannot be answered by the available data.

Fig. 11 shows, moreover, the evolution of bands when switching off NH<sub>3</sub> from a H<sub>2</sub> containing feed at different temperatures. At all temperatures, the spectra are dominated by nitrates with bands at 1551, around 1585, 1612 and around 1304 cm<sup>-1</sup>. The amount of adsorbed species decreases with increasing temperature as indicated by fewer and smaller peaks at higher temperatures. When the ammonia is switched off from the feed containing H<sub>2</sub> at 150 °C the bands assigned to NH<sub>3</sub> and NH<sub>4</sub><sup>+</sup> species on the surface decrease while the nitrate bands around 1615, 1585, 1551 and 1301 cm<sup>-1</sup> increase. This evolution of the bands is similar to the case without H<sub>2</sub> in the feed. At 300 °C, only the nitrate band at 1585 cm<sup>-1</sup> increases, while the other nitrate bands are stable or decrease. At even higher temperatures, all NH<sub>x</sub> bands are very tiny or hardly visible while all nitrate bands clearly decrease showing that the addition of H<sub>2</sub> to the feed has an influence on γ-Al<sub>2</sub>O<sub>3</sub> without silver. For this observed effect of hydrogen at high temperatures (400 and 500 °C) there are two reasonable explanations: hydrogen may either itself reduce the nitrates as observed by [26,31,46] on Ag/Al<sub>2</sub>O<sub>3</sub> or it partially reduces some of the NO<sub>2</sub> to NO which in turn can reduce nitrates to nitrites (reaction (13)). Moreover, less new nitrates will be formed on the catalyst surface when the NO<sub>2</sub> concentration is decreased by partial reduction to NO.

### 3.3. DFT calculations

#### 3.3.1. Oxidation of NO to NO<sub>2</sub> and NO<sub>3</sub> on the surface of transition metals

Fig. 12 shows the potential energy surface diagram for the absorption of NO and O<sub>2</sub> leading to NO<sub>x</sub>, i.e., NO<sub>2</sub> and NO<sub>3</sub> calculated for 6 different transition metal catalysts Ag, Cu, Pd, Pt, Rh and Ru.

For all six different transition metal catalysts both the (111) terrace surface model and (211) step surface model were investigated and the results are similar for both surfaces. The diagram shows that among the transition metals studied the formation of NO<sub>2</sub> on (111) terraces is favorable for both Ag and Cu, whereas the formation of NO<sub>3</sub> is favorable only on Ag. On (211) step surface the formation of NO<sub>2</sub> and NO<sub>3</sub> via oxidation of NO is significantly favorable only on Ag. For other metals NO adsorption without oxidation to NO<sub>x</sub> is preferred. That supports the idea of Ag being necessary catalyst component for the oxidation of NO to NO<sub>x</sub> species as potentially first step of NO SCR.

#### 3.3.2. Adsorption of NO<sub>x</sub> and HNO<sub>x</sub> on the step γ-Al<sub>2</sub>O<sub>3</sub> surface

The model of the step on the γ-Al<sub>2</sub>O<sub>3</sub> (representing uncoordinated Al sites) was used for calculations of NO<sub>x</sub> adsorption energy as the most abundant surface of γ-Al<sub>2</sub>O<sub>3</sub> crystals is the step surface [24]. It has been demonstrated by Mei et al. [33] that NO<sub>3</sub> adsorbs rather strongly on the γ-Al<sub>2</sub>O<sub>3</sub> (100) and γ-Al<sub>2</sub>O<sub>3</sub> (110) surfaces than compared to NO and NO<sub>2</sub>.

A clear decrease of concentration of surface nitrates has been observed by FTIR after addition of hydrogen at high temperatures (experiments at 400 and 500 °C in the Section 3.2.4). Such removal of strongly bound nitrates which block the alumina surface can partly explain the positive effect of H<sub>2</sub> on the activity of Ag/Al<sub>2</sub>O<sub>3</sub> catalysts in NO<sub>x</sub> SCR.

Though authors of [33] have done extensive calculation for the adsorption of NO<sub>x</sub> on γ-Al<sub>2</sub>O<sub>3</sub> (100) and γ-Al<sub>2</sub>O<sub>3</sub> (110) surfaces, however, no effect of H<sub>2</sub> on the stability of surface nitrates on γ-Al<sub>2</sub>O<sub>3</sub> has been considered.

We have calculated the adsorption energy of NO<sub>3</sub> and HNO<sub>3</sub> on our model γ-Al<sub>2</sub>O<sub>3</sub> step surface representing uncoordinated Al surface sites. Five different uncoordinated Al sites are present

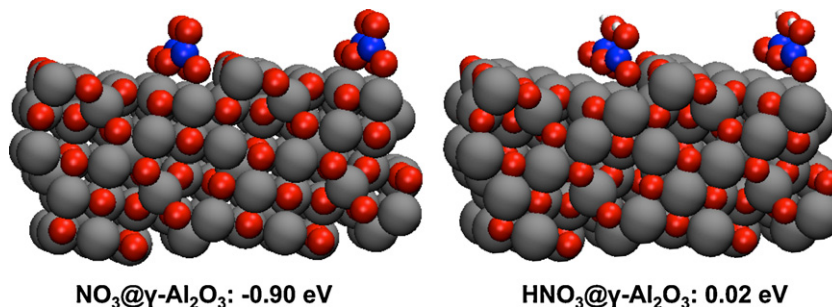


**Fig. 13.** NO<sub>3</sub> and HNO<sub>3</sub> adsorption geometries and adsorption energies on the model step closed packed gamma alumina surface. All the adsorption energies are given with the reference to the gas phase zero energy points of the respective species.

in our model alumina surface as derived from the bulk  $\gamma\text{-Al}_2\text{O}_3$  geometry in [24]. These have all been used for the calculations, however, only the most energetically favorable (energy minimum among studied) adsorption geometries with two oxygen atoms of  $\text{NO}_3$  and  $\text{HNO}_3$  bridging with two Al sites of  $\gamma\text{-Al}_2\text{O}_3$  are reported here. See supplementary information for more details on the used geometries.

The calculated adsorption energy of  $\text{HNO}_3$  (Fig. 13) on the model surface of  $\gamma$ -alumina is considerably smaller than that of  $\text{NO}_3$  (which agrees with [33]), which increases the probability of  $\text{HNO}_3$  removal from the alumina surface compared to  $\text{NO}_3$  in the absence of hydrogen. This supports the suggestion of  $\text{H}_2$  facilitating removal of strongly bound  $\text{NO}_3$  from the alumina.

The mechanism of reduction of adsorbed  $\text{NO}_x$  species by hydrogen with the formation of  $\text{N}_2$  has been previously suggested for  $\text{Pt}/\text{MgO}\text{-CeO}_2$  catalysts for  $\text{H}_2\text{-SCR}$  of  $\text{NO}_x$  [20,21]. This mechanism includes dissociative adsorption of hydrogen on the metal nanoparticle, spillover of the formed atomic hydrogen on the support to the two neighboring  $\text{NO}_x$  species and their reduction with subsequent release of surface sites. However, this is not a major pathway of the SCR in our case because SCR in the absence of  $\text{NH}_3$  is insignificant (Fig. 3, dotted line). Here we suggest that atomic hydrogen reacts rather with a single nitrate or nitrite group with subsequent release of  $\text{HNO}_x$  and adsorption sites on alumina. The evolved  $\text{HNO}_x$  can recombine with the formation of water and nitrogen oxides.

#### 4. Conclusions

Ag supported on  $\gamma\text{-Al}_2\text{O}_3$  is a very promising catalytic system which can be used for the removal of nitrogen oxides from the exhaust of diesel engines in the presence of  $\text{H}_2$ . It is vital that both Ag and alumina are present in the catalyst formulation. The primary role of Ag is the  $\text{H}_2$ -assisted oxidative activation of NO and the reaction of oxidised NO and  $\text{NH}_3$  can proceed further on alumina. Hydrogen also facilitates removal of nitrates from the alumina surface, as supported by DRIFTS experiments and DFT calculation.

The studied catalysts facilitate  $\text{NO} + \text{NO}_2$  mixture reduction without  $\text{H}_2$  in the feed with the  $\text{Al}_2\text{O}_3$  support defining the catalytic activity. Therefore, tuning the alumina support, not only the metal, is vital for obtaining active  $\text{Ag}/\text{Al}_2\text{O}_3$  catalyst.

#### Acknowledgements

This work was supported by grant 09-067233 from The Danish Council for Strategic Research. TEM images were acquired with the support of Center for Electron Nanoscopy (DTU CEN) and personally by Thomas W. Hansen. We acknowledge the supply of the commercial alumina for the study by the SASOL Germany.

The authors also wish to thank Dr. Alexander Yu. Stakheev and Dr. Jakob Weiland Høj for fruitful discussions.

#### Appendix A. Supplementary data

Supplementary data associated with this article can be found, in the online version, at doi:10.1016/j.apcatb.2011.11.042.

#### References

- [1] T.V. Johnson, Int. J. Engine Res. 10 (2009) 275–285.
- [2] S. Subramanian, R.J. Kudla, W. Chun, M. Chatth, Ind. Eng. Chem. Res. 32 (1993) 1805–1810.
- [3] T. Miyadera, Appl. Catal. B 2 (1993) 199–205.
- [4] G.E. Marnellos, E.A. Efthimiadis, I.A. Vasalos, Appl. Catal. B 48 (2004) 1–15.
- [5] Z.M. Liu, K.S. Oh, S.I. Woo, Catal. Lett. 106 (2006) 35–40.
- [6] S. Satokawa, J. Shibata, K. Shimizu, S. Atsushi, T. Hattori, Appl. Catal. B 42 (2003) 179–186.
- [7] R. Burch, J.P. Breen, C.J. Hill, B. Krutzsch, B. Konrad, E. Jobson, L. Cider, K. Eranen, F. Klingstedt, L.E. Lindfors, Top. Catal. 30–31 (2004) 19–25.
- [8] M. Richter, U. Bentrup, R. Eckelt, M. Schneider, M.M. Pohl, R. Fricke, Appl. Catal. B 51 (2004) 261–274.
- [9] M. Richter, R. Fricke, R. Eckelt, Catal. Lett. 94 (2004) 115–118.
- [10] K.-i. Shimizu, A. Satsuma, Appl. Catal. B 77 (2007) 202–205.
- [11] H. Kannisto, X. Karatzas, J. Edvardsson, L.J. Pettersson, H.H. Ingelsten, Appl. Catal. B 104 (2011) 74–83.
- [12] S. Bensaid, E.M. Borla, N. Russo, D. Fino, V. Specchia, Ind. Eng. Chem. Res. 49 (2010) 10323–10333.
- [13] T. Johannessen, H. Schmidt, US patent 2010/0021780 A1.
- [14] C.H. Christensen, R.Z. Sørensen, T. Johannessen, U.J. Quaade, K. Honkala, T.D. Elmøe, R. Køhler, J.K. Nørskov, J. Mater. Chem. 15 (2005) 4106–4108.
- [15] A. Klerke, C.H. Christensen, J.K. Nørskov, T. Vegge, J. Mater. Chem. 18 (2008) 2304–2310.
- [16] V.A. Kondratenko, U. Bentrup, M. Richter, T.W. Hansen, E.V. Kondratenko, Appl. Catal. B 84 (2008) 497–504.
- [17] K.-i. Shimizu, A. Satsuma, J. Phys. Chem. C 111 (2007) 2259–2264.
- [18] E. Kondratenko, V. Kondratenko, M. Richter, R. Fricke, J. Catal. 239 (2006) 23–33.
- [19] P.G. Savva, C.N. Costa, Catal. Rev. – Sci. Eng. 53 (2011) 91–151.
- [20] C.N. Costa, A.M. Efstathiou, J. Phys. Chem. C 111 (2007) 3010–3020.
- [21] P.G. Savva, A.M. Efstathiou, J. Catal. 257 (2008) 324–333.
- [22] E. Ménendez-Porquín, G. Gutiérrez, Phys. Rev. B 72 (2005) 35116–35119.
- [23] B. Hammer, L.B. Hansen, J.K. Nørskov, Phys. Rev. B 59 (1999) 7413–7421.
- [24] M. Digne, P. Sautet, P. Raybaud, P. Euzen, H. Toulhoat, J. Catal. 226 (2004) 54–68.
- [25] P. Sazama, L. Čapek, H. Drobná, Z. Sobálik, J. Dědeček, K. Arve, B. Wichterlová, J. Catal. 232 (2005) 302–317.
- [26] K.-i. Shimizu, J. Shibata, A. Satsuma, J. Catal. 239 (2006) 402–409.
- [27] V. Houel, P. Millington, R. Rajaram, A. Tsolakis, Appl. Catal. B 77 (2007) 29–34.
- [28] G. Madia, M. Koebel, M. Elsener, A. Wokaun, Ind. Eng. Chem. Res. 41 (2002) 3512–3517.
- [29] A. Grossale, I. Nova, E. Tronconi, D. Chatterjee, M. Weibel, J. Catal. 256 (2008) 312–322.
- [30] J.H. Lee, S.J. Schmieg, S.H. Oh, Appl. Catal. A 342 (2008) 78–86.
- [31] F.C. Meunier, J. Ross, Appl. Catal. B 24 (2000) 23–32.
- [32] J.G.M. Brandin, L.H. Andersson, C.U.I. Odenbrand, Acta Chem. Scand. 44 (1990) 784–788.
- [33] D. Mei, Q. Ge, J. Szanyi, C.H.F. Peden, J. Phys. Chem. C 113 (2009) 7779–7789.
- [34] A.A. Tsyganenko, D.V. Pozdnyakov, V.N. Filimonov, J. Mol. Struct. 29 (1975) 299–318.
- [35] J.B. Peri, J. Phys. Chem. 69 (1965) 231–239.
- [36] A.A. Davydov, Infrared Spectroscopy of Adsorbed Species on the Surface of Transition Metal Oxides, John Wiley & Sons, Chichester, New York, Brisbane, Toronto, Singapore, 1984.
- [37] G. Busca, H. Saussey, O. Saur, J.C. Lavalle, V. Lorenzelli, Appl. Catal. 14 (1985) 245–260.
- [38] A. Iglesias-Juez, A.B. Hungria, A. Martínez-Arias, A. Fuerte, M. Fernandez-Garcia, J.A. Anderson, J.C. Conesa, J. Soria, J. Catal. 217 (2003) 310–323.
- [39] S. Tamm, H.H. Ingelsten, M. Skoglundh, A.E.C. Palmqvist, J. Catal. 276 (2010) 402–411.
- [40] S. Tamm, H.H. Ingelsten, A.E.C. Palmqvist, J. Catal. 255 (2008) 304–312.
- [41] S. Kameoka, Y. Ukiisu, T. Miyadera, Phys. Chem. Chem. Phys. 2 (2000) 367–372.
- [42] F.C. Meunier, J.P. Breen, V. Zuzaniuk, M. Olsson, J.R.H. Ross, J. Catal. 187 (1999) 493–505.
- [43] K.I. Hadjiivanov, Catal. Rev. Sci. Eng. 42 (2000) 71–144.
- [44] G.G. Ramis, G. Busca, V. Lorenzelli, P. Forzatti, Appl. Catal. 64 (1990) 243–257.
- [45] M. Schraml-Marth, A. Wokaun, A. Baiker, J. Catal. 138 (1992) 306–321.
- [46] H. Kannisto, H.H. Ingelsten, M. Skoglundh, Top. Catal. 52 (2009) 1817–1820.